

BATSE Observations of Gamma-Ray Burst Tails

Valerie Connaughton¹

NASA Marshall Space Flight Center AL 35812

Received _____; accepted _____

accepted for publication in *Astrophysical Journal*

arXiv:astro-ph/0111564v1 29 Nov 2001

¹work performed while National Research Council Research Associate

¹valerie@msfc.nasa.gov

ABSTRACT

With the discovery of low-energy radiation appearing to come from the site of gamma-ray bursts in the hours to weeks after the initial burst of gamma rays, it would appear that astronomers have seen a cosmological imprint made by the burster on its surroundings. I discuss in this paper the phenomenon of post-burst emission in BATSE gamma-ray bursts at energies traditionally associated with prompt emission. By summing the background-subtracted signals from hundreds of bursts, I find that tails out to hundreds of seconds after the trigger may be a common feature of long events (duration greater than 2s), and perhaps of the shorter bursts at a lower and shorter-lived level. The tail component appears independent of both the duration (within the long GRB sample) and brightness of the prompt burst emission, and may be softer. Some individual bursts have visible tails at gamma-ray energies and the spectrum in at least a few cases is different from that of the prompt emission. Afterglow at lower energies was detected for one of these bursts, GRB 991216, raising the possibility of afterglow observations over large energy ranges using the next generation of GRB detectors in conjunction with sensitive space or ground-based telescopes.

Subject headings: gamma-ray bursts, afterglows

1. Introduction

Afterglow radiation at wavelengths from radio to X-rays has now been seen in several gamma-ray bursts (GRB) detected with Beppo-SAX and the Burst and Transient Source Experiment (BATSE) (e.g. (Costa et al. 1997; Piro et al. 1998; van Paradijs et al. 1997)). This has allowed the unambiguous determination of the cosmological distance scale

of the bursters, has led to the association of gamma-ray bursts with faint galaxies rich in star-forming regions, and has opened up the possibility of using GRBs as cosmological probes (Lamb & Reichart 2000). It has also been a vindication of fireball models for the production of GRBs. The fireball expands relativistically when large amounts of bulk kinetic energy are imparted to a small volume of plasma. Gamma rays are released during the fireball expansion and afterglow synchrotron radiation is anticipated as a result of the interaction between this fireball and the material through which it is moving.

Afterglow radiation is detected when a previously unknown and fading source is seen at a location consistent with the occurrence of a GRB. It is clear that there is a frequency-dependent temporal decay to the afterglow emission and a variety of afterglow temporal and spectral signatures have been seen. The GRBs for which afterglows have been detected encompass a wide range of brightnesses and durations in prompt gamma-ray emission. Indeed, there does not even appear to be a relationship between the brightness of the initial GRB and the brightness or decay time of the afterglow emission. It is tantalizing to scientists that no afterglow has been seen from the class of short GRBs defined as those lasting less than 2 s.

Prompt emission at gamma-ray energies was detected with BATSE (Fishman et al. 1989), and is seen with the Beppo-SAX GRB Monitor (GRBM) (Frontera et al. 1991), Ulysses (Hurley et al. 1992), HETE (Vanderspek et al. 1999) and other dedicated GRB detectors. Prompt X-ray emission can be seen by the Wide-Field Cameras (WFC) on SAX (Jager et al. 1997) and HETE (Vanderspek et al. 1999) or serendipitously by the RXTE All-Sky Monitor (Smith et al. 1999). The first and to-date most successful method used to pin down the afterglow radiation from GRBs has been to slew the Narrow-Field Instruments (NFI) on the Beppo-SAX satellite to observe a location from which the GRBM and WFC detected the prompt emission. The NFI observations are typically made 6 to

8 hours after the GRB trigger. A detection of X-ray afterglow using the NFI provides a location on the sky accurate enough for a search for optical afterglow using the most sensitive telescopes. These optical searches start about 1 day after the GRB trigger. Optical searches have also been initiated as a result of follow-up observations by RXTE which typically start 3–4 hours after the GRB trigger Takeshima et al. (1998).

Gaps exist between prompt and delayed emission observations and their relationship is still unclear. Shock models for GRBs suggest that the initial photons come from collisions of relativistic shells of differing Lorentz factors initiated by some kind of central engine (Rees & Meszáros 1994), while the afterglow is a result of the shock formed by these shells colliding with an external medium (Sari & Piran 1997). It has been suggested in the case of GRB 970228 that if one extends the light curve of the X-ray afterglow back in time, it joins smoothly with the prompt X-ray emission. This may indicate that some of the emission which appears to be part of the prompt component is consistent with being afterglow radiation (Costa et al. 1998). It is difficult to make this argument for bursts in general: the later peaks in bursts do not seem to be significantly different from the initial ones, and not all bursts are multi-episodic. The argument does open, however, the possibility that some component in the late prompt emission might be related to the afterglow. One can then ask what does this component look like, when does it start and how long does it last? Sari & Piran (1999) predict that the early afterglow of short GRBs will be separated from the prompt emission by dozens of seconds, while in longer bursts the afterglow will overlap the initial burst. In their scenario, short bursts are produced by internal shocks between thin shells, longer bursts by thicker shells. Recently, Fenimore & Ramirez-Ruiz (2000) have proposed that the prompt and afterglow gamma-ray emission may overlap if a shell of prompt photons is decelerated by the external medium prior to being caught up by other shells produced by the central engine.

In the work presented here, I explore the period of time from the BATSE GRB trigger to 2000 s later using data between 20 keV and 2 MeV. This time window is not usually probed in afterglow observations because of the delays in obtaining good GRB locations and mobilizing observing facilities. The continuous BATSE data stream and the development of a suitable background subtraction technique make possible the examination of long-term, low-level emission at gamma-ray energies. This technique will be described, followed by the results of its application to a search for long-lived emission in individual events and also in the combined signal from hundreds of events.

2. BATSE measurements of GRB tails

BATSE recorded continuously with all 8 Large Area Detectors (LADs) background data with 16 energy channel, 2.048 s time resolution for the $\sim 80\%$ of the time during which the detector voltages were activated (they are disabled during South Atlantic Anomaly (SAA) passages), and the spacecraft was in contact with a TDRSS satellite. Over the ~ 5600 s spacecraft orbital period, large, energy-dependent variations in background count rates are registered with the LADs owing to passage through regions of differing magnetospheric activity. Variations also occur in the cosmic ray component of the background rates because of changing rates of decay of induced radioactivity in different magnetic fields. A variation by a factor of about 1.4 in count rates occurs in a typical orbit. The triggering requirement for BATSE of 5.5σ above the rates between 50 and 300 keV registered during the previous 17 s in 2 or more of the 8 detectors in 64, 256, or 1024 ms ensures that the system responds to sudden increases in count rates typical of the prompt gamma-ray emission of GRBs. These increases (triggers) are easily distinguished above variations in background rates. In contrast, GRB afterglows at lower energies have typically been smooth on time-scales of thousands of seconds. To ensure detection of a similar trend at higher energies, careful

background subtraction is required to extract any subtle signal over these time-scales in the BATSE system.

2.1. Background subtraction in the BATSE data

In addition to the background variation pattern over each orbit, successive orbits are quite different owing to the Earth’s rotation. The spacecraft orbit precesses, with a period of about 50 days, so that at the same time on two successive days, the spacecraft latitudes will have shifted. The closest match in rates registered by the LADs occurs at times 15 orbits before and 15 orbits after the orbit of interest. A background measurement is obtained by using the average of the count rates from two orbits, each 15 orbital periods away from the time of interest when a GRB triggers the instrument.

Figure 1 (left, top) shows the three superimposed lightcurves from a stretch of time covering two orbits on three successive days. One lightcurve is centered on GRB 970508, the other 2 are centered on times 15 orbits before and after the time of trigger of GRB 970508 and are to be used to estimate the background before, during and after the burst. In Figure 1 (left, bottom) the average of the background curves has been subtracted. It can be seen that in addition to the triggered event at time $t = 0$, there are noise events in the orbits which are not constant from one to the next. The most significant of these discrepancies occur when the spacecraft exits or enters the SAA. These and other mismatches (electron events, phosphorescent spikes) are flagged and removed in the analysis, resulting in the case of GRB 970508 in the profile shown in Figure 1 (right). The holes in the light curve arise from telemetry gaps, disabling of the instrument during passage through SAA, and the exclusion of data from times during which the burst position is occulted by the Earth. In order to obtain a background measurement in this fashion there must be no spacecraft re-orientation during the 3 days so that the detector geometry relative to the burst position

is constant. Telemetry gaps must not occur at the time of the burst or at the corresponding background orbit centers, and an additional requirement of no GRB triggers during the background orbits is imposed.

The quality of this background fitting was assessed using test orbits (which contain no triggered events) centered at a time 5 orbital periods after or before a GRB trigger. The test signal comprised the sum of the count rates from the detectors which were triggered by the GRB at times when the GRB position was visible to the spacecraft (i.e. not Earth-occulted). Test background orbits were found on adjacent days separated in time by 15 orbital periods, and the flatness of the resulting light curve after background subtraction and cleaning was taken as a measure of the power of the technique. It was found that the light curves were flat, but that non-Poissonian errors were present, particularly in the lower energy channels and at high spacecraft geomagnetic latitudes. Slight mismatches in the rates (probably due to spacecraft precession, and also due to the noisier data at the peaks of the orbits) are more severe at very high or very low latitudes than at the equator. A systematic error was added to the counting error, the magnitude of which depended on the latitude of the spacecraft. For each energy channel the systematic error was 10% of the deviation of the background rate from the average (i.e. at the equator) background rate.

For an individual orbit, the sensitivity of this technique is estimated to be of the order of 10^{-9} erg cm⁻²s⁻¹, or an order of magnitude lower than the BATSE trigger threshold. The technique has been successfully applied when examining the possible presence of tails in the bright gamma-ray burst GRB 980923 (Giblin et al. 1999). In the case of GRB 980923 the traditional method of background subtraction by linear interpolation of intervals before and after the GRB failed owing to the duration of the tail, the variations in background levels, and the faintness of the signal in the tail. This tail signal was more than two orders of magnitude fainter than the bright peaks which precede it, and persisted for at least

200 s whereas the main event stopped suddenly after 20 s. Other bursts have been seen which exhibit bright spikes superimposed on tail-like emission, but none with so dramatic a transition as GRB 980923. If this tail-like emission is a feature of GRBs in general, then it occurs at a level which is too faint to be visible by BATSE in most individual bursts, but might be detectable in the combined signal from many events. In such an analysis, it is crucial that the addition of signal not be hindered by an inadequate treatment of background count rates. The robustness of the orbital background subtraction method developed here to signal stacking was assessed by summing the background-subtracted test orbits described above. Of 100 original test orbits, 35 were rejected for poor background fits - either visually or in a chi-squared test performed on data between -6000 and -4000 s, and 4000 and 6000 s from the center of the test orbit. Figure 2 shows the summed light curve of the remaining 65 test orbits from 1000 s before to 1000 s after the aligned centers of the test orbits. The light curve is best fit by a line of vertical offset -0.5 ± 0.7 counts s^{-1} event $^{-1}$, consistent with zero (dotted line).

Having established the flatness of the residual light curve after background subtraction and summation of light curves in the absence of GRB triggers, background-subtracted signals for orbits centered on triggered GRBs were summed, aligning the light curves at the peaks of the GRBs as Mitrofanov et al. (1996) did in their analysis of the asymmetry of burst peaks. The count rates in each 2.048 s time bin in the orbits before and after the GRB trigger during which the burst location was not Earth-occulted and for which data exist for all three days were included in the summed light curve. Ideally, the combined light curve would be a sum of all GRBs detected by BATSE, but the event attrition rate was quite severe owing to the data-intensive orbital background subtraction. BATSE triggered on 2365 cosmic GRBs between 1991 April and 1999 March. Of these, 526 occurred within 15 orbits of a spacecraft reorientation so that at least one of the two orbits required for background subtraction had a different detector geometry from that at the time of the

GRB trigger and could not be further analysed. A further 595 were rejected because of the presence of a GRB trigger in one of the two background orbits. 427 GRBs triggered in a telemetry gap (special burst data is stored at these times but the continuous data stream is unavailable), or a telemetry gap or SAA passage was in progress at $t = 0$ of at least one of the background orbits. These events were excluded owing to the lack of data around the time of the trigger. Background fits for 296 of the remaining 816 events were found to be unsatisfactory using a χ^2 test so that in total, 520 BATSE GRBs were available for inclusion in the combined light curve.

Durations of GRBs detected with BATSE range from milliseconds to hundreds of seconds. The distribution of these durations is clearly bimodal (Kouveliotou et al. 1993) with a duration of 2s separating the short from the long GRBs. Efforts to associate the two classes with separate populations have generally been unsuccessful, although the bursts in the long part of the distribution do appear spectrally softer than the short ones (Kouveliotou et al. 1993). The most recent distinction between the two classes has been the lack of afterglow emission detected for the short ones. This lack cannot conclusively be claimed as an absence of afterglow intrinsic to short GRBs, since no short bursts have been seen by the WFCs on Beppo-SAX, and no sensitive counterpart searches have, therefore, been undertaken. About 80% of bursts seen with BATSE are in the long part of the distribution, and this holds for the sample of 520 bursts analysed here. The long and short bursts are treated separately in order to answer the following questions: Do long bursts in general show evidence for tail emission such as that seen in GRB 980923 but at levels below what would be visible in individual events? Can any such tail emission be seen at equally low levels in the combined signal from short GRBs?

3. Results

3.1. Long Bursts

Figure 3 shows the combined light curve for the 400 long bursts. The times are logarithmic and given relative to the aligned peak, t_0 , and the rates are summed above 20 keV and averaged by dividing the total rates in a time bin by the number of bursts contributing to that bin. The time axis starts at $t_0 + 40$ s. Bursts with precursor or successor emission, defined as outbursts which are separated from the time of the peak by longer than the duration of the longest episode of the burst, are excluded. This exclusion is performed because these multi-episodic events can sometimes have episodes of almost equal intensity so that deciding which peak to place at $t = 0$ becomes problematic.

There are regions of the orbit following a trigger which are not well-sampled - it is very likely, for example, that a burst position will be occulted 2000 s after its detection. Since only bursts which trigger outside of gaps in the spacecraft telemetry are analysed, the likelihood of a telemetry gap or an SAA passage also increases with time. The statistics of the combined light curve are, therefore, better closer to $t = 0$, partly because the signal is larger, but also because more bursts contribute to the averaged count rates. The ill-sampled light curve bins are eliminated by excluding time bins where more than 75% of the burst positions from a sample of bursts are occulted or occur in telemetry gaps.

No tail-like excess is seen in the hundreds of seconds before the aligned peak, and rates have returned to background following the ill-sampled portions of the orbit which end at about $t+4000$ s. The period of interest is that which occurs during and after the prompt emission. It can be seen that the summed light curve exhibits a tail-like low-level of emission which extends beyond the duration of most GRBs. The tail extends to at least several hundred seconds after the aligned peak, and may still be there in the time bins

between 1000 and 2000 s after t_0 . Although most long bursts last only tens of seconds, and those with the longest measured durations are generally of the multi-episodic variety which were excluded from this light curve, it is reasonable to worry about the tail being a reflection of the duration of the longest bursts in the sample. The 400 long bursts were divided into two groups according to their durations, and a medium duration subsample defined as shortest 50% of long events was created which contains 200 bursts with durations greater than 2 s but less than 30 s. Figure 4 starts at $t_0 + 40$ s and shows on a logarithmic scale the count rates per burst in the long burst sample and the medium sample: the stars are the 400 bursts longer than 2 s, the triangles are those 200 medium duration bursts, whose main prompt emission is deemed to be over by the time of the start of the plot. Count rates per burst between 20 keV and 100 keV are shown in the left plot, and are given as a fraction of the peak count rates at t_0 on the right. The tail is visible in both duration groups, although the count rates are higher for the longer bursts until $t_0 + 200$ s since the longest bursts are still contributing prompt emission at this time. The contribution to the tail beyond this time is independent of burst duration, suggesting a component is being detected which is distinct from the prompt emission. If the emission seen from the 200 medium duration bursts is mostly tail emission from $t_0 + 40$ s onward, then the average appearance of the tail is that shown by the triangles in Figure 4 and can be fit by a power law of index 0.6 ± 0.1 . It is probable, however, that like most burst and afterglow properties, this tail varies considerably in individual bursts.

The spectrum of the emission in the combined light curve of Figure 4 is characterized by the ratio of counts detected in two adjacent energy channels. Figure 5 shows the evolution in time of the hardness of emission, measured as the ratio of the counts between 50 and 100 keV to those between 20 and 50 keV sample, starting at 10 s after t_0 . The stars show the summed complete long GRB sample exhibiting a general softening which steepens with time after about $t_0 + 200$ s until $t_0 + 600$. The triangles indicate the trend for the

summed medium duration bursts where emission beyond $t_0 + 20$ s is flat at first and then follows the softening trend seen in the longer bursts. The final point, which is the hardness ratios from the summed counts in the two bins at and above 1000 s in Figures 3 and 4 indicates a hardening in both sets of bursts, though statistics are poor at these low flux levels. This hardening is seen in the subset of the 182 longest bursts (excluding the medium duration GRBs) so it does not seem to be a contribution made solely by medium duration bursts.

Division of the 400 long bursts into three brightness-selected groups indicates that the tail is measured in the summed light curves of even the dimmest group. Figure 6 shows the intensity of the tail for the 3 groups, the stars showing the brightest group (peak flux > 1.5 photons $\text{cm}^{-2}\text{s}^{-1}$ on a 1 s time-scale), the squares pertaining to the dimmest bursts (< 0.65 photons $\text{cm}^{-2}\text{s}^{-1}$ at the peak intensity) and the triangles to those of intermediate brightness. Each group contains 133 bursts. The intensity of the tail as a fraction of the peak intensity (count rates at t_0) for each subsample is shown in the right hand plot of Figure 6. Although the magnitude of the tail appears largest in the bright group, the fraction of the peak count rate in the tail is smaller than in the dimmer groups. The similarity of the tail in the three groups despite the variety of bursts to which they pertain may lead to worry about the tail being an artifact of the orbital background subtraction method. It is clear from the flatness of the summed test orbits in Figure 2, however, that no such feature is introduced by this methodology.

3.2. Short Bursts

Figure 7 shows the combined light curve for the 100 short bursts - those with durations less than 2 s - and starts at $t_0 + 10$ s. Although the post-burst emission is not as prominent as in the summed signals from the longer burst, an excess is apparent from $t_0 + 20$ s out to

$t_0 + 40$ s and maybe even in the time period between $t_0 + 100$ s to $t_0 + 300$ s. The level of tail emission per contributing burst is a factor of 3–4 smaller than for the long bursts at this time, and the error bars are larger owing to the smaller sample size, so that fitting this tail emission to a power-law or other model of decay is not meaningful. Likewise, the flux is not large enough to compare its spectrum to the prompt emission or track any changes in hardness ratios through the period of the excess. This lightcurve is, however, less flat than would be expected from the light curve obtained with the test orbits shown in Figure 2.

3.3. Individual Bursts

Long-lived gamma-ray emission is detected in the combined signal from many GRBs in the long part of the bimodal distribution and does not seem to scale with the brightness and duration of the prompt emission. Some individual bursts have visible persistent low-level emission following a much brighter episode, and in the class of bursts known as FREDs (Fast Rise Exponential Decay) the prompt emission decays gradually as a power-law in time. The orbital background subtraction method described above reveals these types of long-lived emission with greater sensitivity and over longer time-scales than are first apparent. The individual light curves from the bursts comprising the long-duration sample described above indicate that some have a more pronounced long-lived component than others, thus contributing more to the combined tail, without any obvious discriminant in the prompt emission to indicate why this might be the case, and not all bursts appear to have a detectable long-lived component. Likewise, afterglows at lower energies have been detected for a variety of GRB brightnesses and durations, but have not been seen for all GRBs for which they were sought. Efforts to correlate the presence of afterglow radiation with some property of the GRB prompt emission have not been successful. The dramatic change in appearance and spectrum seen in GRB 980923 and reported by Giblin et al.

(1999) suggests that distinct emission components may be present in some GRBs. If the long-lived, low-level emission seen in GRB 980923 is related to the afterglow rather than the prompt emission of this burst, then one might expect some correlation between the detection of gamma-ray tail emission and the detection of lower-level afterglow emission.

Between 1996 July and 1999 December a total of 45 well-located GRBs were followed up in a search for afterglow emission at X-ray, optical, infrared or radio wavelengths, with varying degrees of depth of observation and delay times. Of this sample, 19 were detected by BATSE and could be processed using the background-subtraction methodology developed here. Although counting statistics and background fluctuations in individual orbits limit the sensitivity to which tails can be sought in individual bursts, each of these 19 events was examined and categorized as being tailless, tailed, possibly tailed, or impossible to categorize owing to poor or ambiguous background fits. Table 1 shows the list of obviously tailless events where the prompt emission stops abruptly and the return to background is immediate, and those where the presence of tailed, long-lived emission is apparent. The Table also indicates the presence of convincing afterglow candidates detected at X-ray (X), optical (O), infrared (I) or radio (R) wavelengths. A “Y” indicates a counterpart, a “N” implies observations were made but no counterpart was found, and the field is left blank if no counterpart searches were completed at a particular wavelength. The afterglow observations listed in Table 1 were taken from van Paradijs, Kouveliotou, & Wijers (2000) who provide a comprehensive list of observations through 1999 July, and from circulars issued to the Global Coordinates Network (Barthelmy et al. 2000).

The most dramatic gamma-ray tail is seen in GRB 991216. Although the tail emission is so faint compared to the peak emission that it cannot be seen without the background-subtraction method developed here, it lasts at least 1100 s, at which time the position becomes Earth-occulted, and may be faintly visible at 4000 seconds after the

occultation period ends. The tail is so bright that an occultation step can be seen in the background-subtracted data at the expected time. The spectrum of the tail is significantly different from the peak emission, and a more detailed analysis of this burst is given in V. Connaughton et al. (in preparation).

Afterglows at all observed energies were seen for GRB 991216, as is also the case for another two tailed events, GRB 980329 and GRB 980703. Only a weak limit can be set by the absence of any counterpart to GRB 971024 because the follow-up optical observations were not very deep, so that the trend of visible tails existing for events with measured afterglows is not seriously compromised by the lack of a counterpart for GRB 971024. The non-detection of even an X-ray afterglow for GRB 970111 has always been puzzling given the brightness of the burst. Any weak correlation one might infer between gamma-ray tails and low-energy afterglows is negated by the presence of a tail in the BATSE data for GRB 970111. The situation is further weakened when one counts among the tailless events the afterglow-rich GRB 971214, and especially GRB 970508 which has such a convincing and much-observed afterglow light curve measured over a long and broad-energy base line.

No correlation can, therefore, be implied between the presence of gamma-ray tails and lower-energy afterglow detection using this small sample of GRBs.

4. Discussion

Emission in gamma rays from long GRBs seems to extend beyond what is first evident, at a level which is low compared to the prompt emission. It appears to overlap the prompt emission and outlast it by more than several hundred seconds, following a smooth decay that can be fit by a power law of index -0.6. Such power-law decays have been seen in the GRB afterglow detections at later times and lower energies, with indices varying between

1.1 and 1.9 (X-ray) and 1.1 and 2.4 (optical) (van Paradijs, Kouveliotou, & Wijers 2000). The results presented here were obtained by summing the background-subtracted signals from 400 GRBs lasting longer than 2 s in order to establish the presence of gamma-ray tail emission in long bursts in general. This tail was also seen in a medium duration sample comprising those 200 bursts lasting between 2 and 30 s. The similarity of the tail in the summed light curve of the medium sample to that of the long sample suggests a lack of correlation between the duration and magnitude of the tail emission and the duration of the prompt GRB episode. The decay power law index of -0.6 is an average value so that if the gamma-ray tail is related to the afterglow at lower energies, one might expect that the variations in decay indices seen at lower energies are also inherent in the gamma-ray tails. In a study modeling the temporal decay of 40 GRBs, Giblin et al. (2000) find a mean power-law of 2.05 ± 0.51 , which is only marginally consistent with this work. One might expect the signal in the combined light curve to be dominated by flatter decays at the later times explored in this analysis (unless there is some dependence of the power-law decay index on the initial brightness of the tail component) but the average decay seen in this analysis is flatter than any single burst modeled in Giblin et al. (2000). This modeling of individual bursts uses data which is closer to the peak emission than in the analysis presented here, and it is possible that the tails in Giblin et al. (2000) may represent a decaying of prompt burst pulses rather than the shape of the gamma-ray afterglow (except for the tail of GRB 980923 which has such a different spectrum from the main emission).

By looking at tail emission as a fraction of the peak flux, one can see that for the ensemble of medium duration bursts whose tails can be measured over a longer time-line than the longer bursts, the emission at $t_0 + 40$ s is about 4/1000 that at the peak, and 1000 s later it is an order of magnitude lower yielding an approximate fluence during this time of 2 photons/cm⁻² above 20 keV, or $\sim 5 \times 10^{-7}$ erg/cm⁻² assuming a mean medium-duration GRB peak flux and a GRB-like power-law spectrum. This compares with an estimate of

the average medium duration burst fluence of $\sim 4 \times 10^{-6}$ ergs/cm⁻² obtained by summing the fluences between 20 and 300 keV for bursts in the sample using values from the BATSE current catalog (<http://gammaray.msfc.nasa.gov>). The observed brightness of a GRB, measured by its peak flux, is affected by its distance to the observer, but the wide range of luminosities implied by the measurements of just a few GRB redshifts suggests a broad intrinsic luminosity function for the population of GRBs (Lamb & Reichart 2000). By dividing the 400 long bursts into 3 groups according to peak flux and examining their summed light curves, it was seen that although the tail emission is most significant in the brightest group, the difference is not as great as the variation in peak fluxes between the ensembles. The fact that there is some dependence of the magnitude of the tail on the GRB peak brightness as seen in the left panel of Figure 6 might be because on average the dimmer bursts are further away. Figure 6 (right) shows, however, that as a fraction of peak count rates the tail is brighter for the dimmer ensemble. This implies a tail component which does not scale directly with the intrinsic brightness of the prompt GRB emission. Whether this tail component is truly independent of the brightness of the prompt emission cannot be inferred from this analysis, but the intensity of the tail is clearly not directly proportional to the intensity of the burst. The average fluences of the prompt emission in the 3 brightness groups obtained as above from the current BATSE catalog are 1.5×10^{-5} , 3.2×10^{-6} , and 1.3×10^{-6} ergs/cm⁻². The count-rate fluences of these groups, calculated between $t_0 + 100$ and $t_0 + 1000$ s (to avoid including much prompt emission) calculated from Figure 6 are 12000, 6000, and 5000 counts. Assuming a similar spectrum in the tails of the 3 brightness groups, the ratio of the fluence in the prompt emission to the fluence in the tail does not follow a linear relationship. The results appear consistent with the fluence in the tail scaling with the square root of the fluence in the prompt emission to within the large errors associated with this crude estimate.

Giblin et al. (1999) and Burenin et al. (1999) have found tail-like emission in the

bright bursts GRB 980923 and GRB 920723, respectively. A temporal decay in time with a power law index of -0.69 ± 0.17 was seen in the case of GRB 920723, consistent with this analysis. A much steeper index of -1.8 ± 0.02 was measured for GRB 980923, illustrating the variety of decays which may be contributing to the combined tail profile. The fluence contained in the tails of bursts GRB 920723 and GRB 980923 is 20% and 7% of the total burst fluence, respectively, which agrees with the estimated fluence in the tail between $t_0 + 40$ s and $t_0 + 1000$ s of 12% of the average prompt GRB fluence for the medium duration sample. One hundred seconds after the peak, the emission of GRB 920723 was 1/1000 that of its maximum flux, that of GRB 980923 was a few thousandths of the peak intensity. The intensity of this tail emission is considerably lower than that at the peak, consistent with what is seen in the analysis presented here, but what really separates it from the main emission is a sharp spectral transition. The tail in each case is much softer than the peak. Clearly, the issue of spectral differences between prompt and tail emission is important in establishing distinctions between the two components. Gamma-ray bursts in general show a softening throughout their light curve (Norris et al. 1986) so that any additional softening which is a signature of a separate component will be hard to discern in the summed signal from many bursts. With the overlap of prompt and tail emission of bursts of different durations and spectral characteristics, it is difficult to separate these components. There is some evidence for distinct spectral components in the main and tail emission which can be seen in the evolution of the hardness ratio of the combined tail signal shown in Figure 5. Softer emission is apparent in the medium duration bursts until $t_0 + 100$ s compared to the entire set of long bursts which contains events which are still in their prompt phase during that time. The flatness of the medium burst set from $t_0 + 20$ to $t_0 + 300$ is consistent with what was seen in the tail of the individual burst GRB 980923. Claims of distinct spectral identities for prompt and tail emission are more convincing, however, in individual bursts where the spectral forms can be modeled rather than using hardness ratios between two

energy bands, and the transition between prompt and tail emission is easier to discern.

A sudden steepening and subsequent flattening of the spectrum seen at $t_0 + 1000$ s in Figure 5 is more puzzling. This effect is seen in both the medium and the long burst data sets. It is difficult to quantify given the low fluxes involved, but qualitatively, at least, this hardening may be consistent with the onset of an Inverse Compton (IC) component which is anticipated by Dermer et al. (2000) (in external shock GRB models); by Totani (1998) (from synchrotron emission by protons in the GRB jet to explain delayed high-energy GRB emission such as that seen in GRB 940217 (Hurley et al. 1994)); and more recently by Panaitescu & Kumar (2000) and Sari & Esin (2001). Sari and Esin state that this inverse Compton component might most easily be seen in the early afterglow at gamma-ray and X-ray energies. Fast-cooling fireball scenarios explored by Sari & Esin (2001) show a significant IC presence in the gamma-ray spectrum 43 minutes after the trigger time. While they expect the onset and importance of the inverse Compton emission to vary from one burst to another, the hardness of the summed rates from all the long (> 2 s) bursts between 1000 and 2000 s after their aligned peak might be indicative of the onset of the IC frequency entering the observable energy range of BATSE and the domination of this IC component over the fading synchrotron tail. At later times in the afterglow, IC emission has been reported by Harrison et al. (2001) as contributing to the X-ray afterglow spectrum of GRB 000926 2 and 10 days after the GRB but no other afterglows have so far been observed with this bump in their afterglow spectrum.

In the analysis of the combined light curve, the most convincing evidence for the distinct nature of the tail relative to the prompt emission is the lack of scaling of its duration and intensity with those of the early emission. If the emission components are distinct, then their overlap in time is consistent theoretically with the deceleration model of Fenimore & Ramirez-Ruiz (2000). This model suggests that bursts from fireballs with

high Lorentz factors will exhibit two contemporaneous emission components, one a result of an initial fireball-external medium deceleration shock, the other the arising from the internal shocks within the fireball. If the Lorentz factor is low (< 1000) internal shocks occur prior to the first shell being decelerated by the external medium, and only main prompt emission and the post-burst afterglow will be seen. The deceleration depends, therefore, on the initial Lorentz factor of the fireball, not on any parameter such as the width of the shells (determining duration of GRB peaks) or the total energy in the fireball (determining GRB intensity and fluence). One signature of such a deceleration phenomenon is an overlapping tail component which is different in nature from the main emission. Fenimore & Ramirez-Ruiz (2000) postulate that this component will be smoother, weaker and spectrally distinct from the main emission. The analysis presented here finds a tail component which could result from this deceleration and the possibility that all long bursts exhibit this property is not excluded. A connection between GRB tail emission and the deceleration model has a major impact on the energetics of GRBs. The appeal of deceleration by an initial external shock is that it makes the internal shocks more efficient by introducing a large difference in Lorentz factors between leading and subsequent fireball shells. Not so much of the bulk energy remains to be dissipated following the prompt GRB episode, lowering the total energy budget at the expense of a high initial Lorentz factor.

If in establishing the distinctness of the prompt and tail gamma-ray components detected here, one looks to lower energy afterglow observations rather than theory, the picture is also encouraging. Afterglows at lower energies have been measured for both bright and dim BATSE events, and for both medium and long-duration bursts, so that the independence of a gamma-ray tail component of both duration and brightness of the prompt emission is not unexpected if this tail component is related to the afterglow emission.

Not all bursts seem to have lower-energy afterglow emission, and not all bursts have

obvious gamma-ray tails. The lack of correlation found here between the detection of afterglow emission at X-ray, optical and radio energies and the presence of a gamma-ray tail in individual events, however, suggests the relationship between the different afterglow components may not be simple. It is not possible to draw conclusions based on the small number of tailed and obviously tailless GRBs. The unambiguous determination of the absence of a gamma-ray tail is often difficult given the sensitivity of the BATSE detectors and the background-subtraction technique. Moreover, the searches for afterglows at lower energies are not always deep or timely enough to place severe limits on afterglow counterparts.

To date, no afterglow emission has been seen from short bursts, but no such bursts have been detected in prompt X-rays with the SAX Wide-Field Cameras and consequently no follow-up observations have been performed for well-localized short events. It is not known whether the lack of detected afterglows from short bursts is a function of their being deficient in prompt X-ray emission, whether instrumental biases result in poor triggering efficiency for these events using the SAX GRBM/WFC system, or whether the smaller numbers of short GRBs have allowed them to elude detection thus far. In this analysis, there does appear to be some excess in the tens of seconds after the summed, aligned peaks of the short GRBs in Figure 3, consistent in onset time with the predictions of Sari & Piran (1999) that the early afterglow of short GRBs will be separated from the prompt emission by dozens of seconds, while in longer bursts the afterglow will overlap the initial burst. The flux at a given frequency at the onset of the afterglow is determined by an initial Lorentz factor. It is conceivable that in these short bursts there is an afterglow signal at gamma-ray energies which is just at the sensitivity of the analysis presented in this paper, but the evidence is more tantalizing than conclusive.

Long-lived tail emission does seem to be a common attribute of long BATSE GRBs.

It is not clear whether tail components are associated with the prompt emission or the afterglow, but the combined light curves from various ensembles of events suggests they are somewhat independent of the duration and intensity of the initial burst of gamma rays. Owing to the overlap in time between the tail and the main emission in individual bursts like GRB 980923 (Giblin et al. 1999) evidence for the distinct natures of the two components comes mainly from spectral differences between them. The most exciting discovery from the analysis of the 19 individual bursts presented here is the tail following the bright burst GRB 991216 for which afterglow candidates were observed at lower wavelengths. V. Connaughton et al. (in preparation) find a preliminary spectral analysis of this burst confirms the hypothesis of distinct components. Detection of high-energy afterglow emission coincident with low energy afterglow observations in individual bursts expands the energy range over which energy-frequency temporal dependencies predicted in blast-wave models for the production of afterglow emission can be probed (Wijers, Rees, & Meszáros 1997). Although BATSE can no longer provide this high-energy platform, HETE and Swift will be operational during the next few years. The observations of GRBs at optical (Swift), X-ray and gamma-ray energies either simultaneously or within seconds of a trigger will avoid the time lag inherent in the pioneering afterglow pursuits of SAX and RXTE which require time-consuming spacecraft repointings. Swift will be sensitive to lower gamma-ray fluxes than BATSE so that tails of individual bursts will be easier to probe. While HETE is not as sensitive, its circular orbit facilitates background subtraction and any long-lived, low-level emission will be easier to discern. Both of these major GRB space missions will be decisive in answering the questions of the prevalence and nature of tails in long GRBs and the possible presence of tails in the short events.

The author thanks an anonymous referee for constructive comments. She is grateful to Re'em Sari and to Tim Giblin, Michael Briggs, Chryssa Kouveliotou, and Matt Scott of the

BATSE team for critical reading of and suggestions for improvements to this paper. She credits Ralph Wijers with the encouragement and nagging which spurred the completion of the paper. The author also acknowledges the National Research Council postdoctoral fellowship program which supported the research presented here.

REFERENCES

- Barthelmy, S. 2000, http://gcn.gsfc.nasa.gov/gcn/gcn_main.html
- Burenin, R. A. et al. 1999, *A&ASupp.*, 138, 443
- Costa, E. et al. 1998, *Proc.4th Huntsville GRB Symp. (AIP CP428)*, eds. C. A. Meegan, R. D. Preece, & T. M.Koshut, 409
- Costa, E. et al. 1997, *Nature*, 387, 783
- Dermer, C. et al. 2000, *ApJ*, 537, 255
- Fenimore, E. E. & Ramirez-Ruiz, E. 2000, submitted to *ApJ* and preprint (astro-ph/9909299)
- Fishman, G. J. et al. 1989, in *Proc. GRO Science Workshop*, ed. W.N. Johnson, 2
- Frontera, F. et al. 1991, *Adv. Space Res.*, 11, 281
- Giblin, T. et al. 1999, *ApJ*, 524, L47
- Giblin, T. et al. 2000, submitted to *ApJ*
- Harrison, F. et al. 2001, *ApJ*, 559, 123
- Hurley, K. et al. 1994, *Nature*, 372, 652
- Hurley, K. et al. 1992, *A&ASupp.*, 92, 401
- Jager, R. et al. 1995, *Adv. Space Res.*, 13, 315
- Kouveliotou, C. et al. 1993, *ApJ*, 413, L101
- Lamb, D. Q. & Reichart, D. E. 2000, *Proc. 5th Huntsville GRB Symp.* eds. G. J. Fishman, R. M. Kippen & R. Mallozzi, (AIP CP 526), p.658

- Mitrofanov, I. G. et al. 1996, ApJ, 459, 570
- Norris, J. P. et al. 1986, ApJ, 301, 213
- Panaiteescu, A. & Kumar, P. 2000, ApJ, 543, 66
- Piro, L. et al. 1998, A&A, 331, L41
- Rees, M. J. & Meszárós, P. 1994, ApJ, 430, L93
- Sari, R. & Piran, T. 1997, ApJ, 485, 270
- Sari, R. & Piran, T. 1999, ApJ, 520, 641
- Sari, R. & Esin, A. 2001, ApJ, 548, 787
- Smith, D. A. et al. 1999, ApJ, 526, 683
- Takehima, T. et al. (1998), Proc. 4th Huntsville Symp., eds.C. A. Meegan, R. D. Preece,
and T. M. Koshut (AIP CP 428), p. 414
- Totani, T. 1998, ApJ, 509, L81
- Vanderspek, R. et al. 1999, A&ASupp, 138, 565
- Van Paradijs, J. et al. 1997, Nature, 386, 686
- Van Paradijs, J., Kouveliotou, C., & Wijers, R. A. M. J. 2000, ARA&A, 38 (in press)
- Wijers, R. A. M. J., Rees, M., & Meszárós, P. 1997, MNRAS, 288, L51

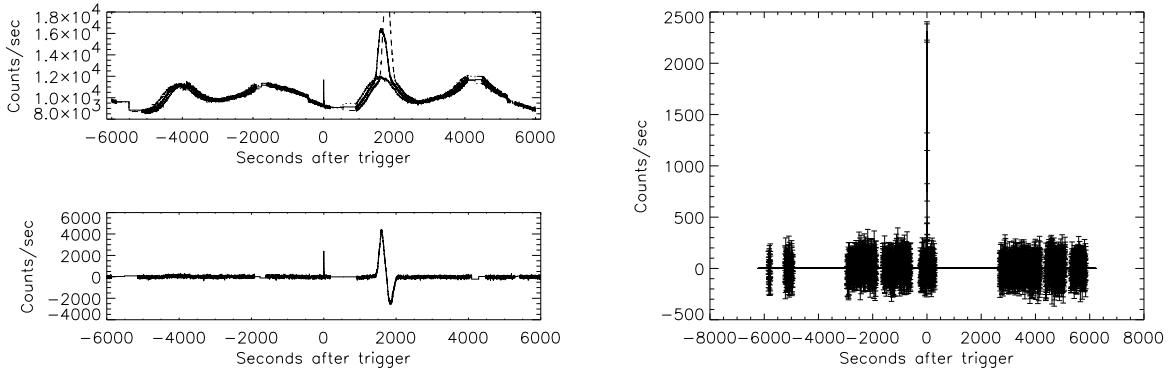


Fig. 1.— 3 superimposed BATSE LAD lightcurves showing the count rates from stretches of time covering two orbits on three successive days, one centered on GRB trigger 6225, the others centered on times 15 orbits before and after the time of trigger which are to be used to estimate the background before, during and after the burst. The top left plot shows the orbits separately, in the bottom left plot the average of the two background light curves is subtracted from the burst light curve. Telemetry gaps and regions of magnetospheric noise (between 1300 and 2000 s) can be seen. On the right hand side, the noisy regions have been removed and only times where the burst location is not Earth-occulted are included. The triggered event can be seen at $t = 0$. The errors shown are statistical.

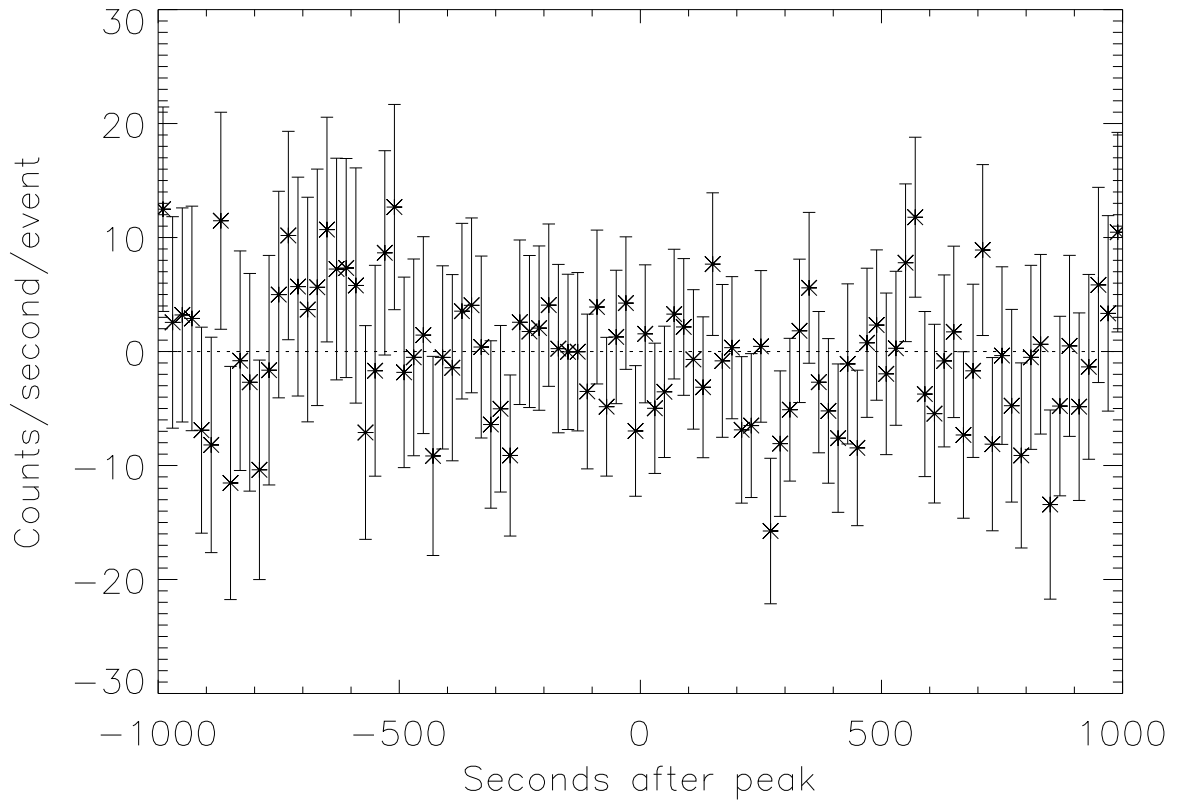


Fig. 2.— Lightcurve for 65 summed background-subtracted test orbits (summed energy channels). The best fit to the light curve is consistent with the zero-level dotted line.

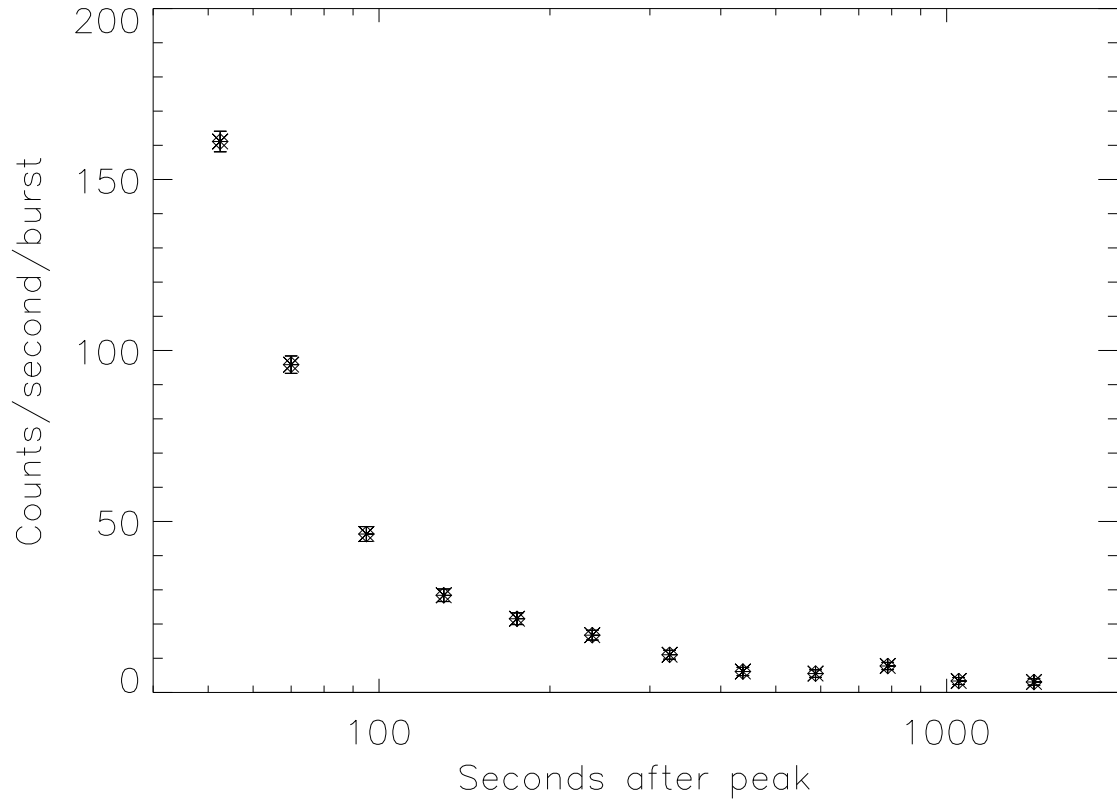


Fig. 3.— Lightcurve for the 400 long (> 2s) summed and background-subtracted BATSE bursts after peak alignment, with peak time suppressed, summed energies.

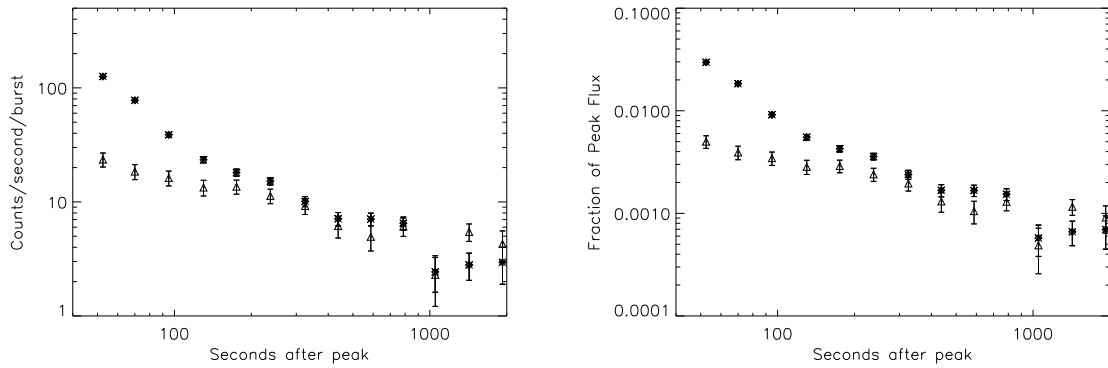


Fig. 4.— Lightcurve for summed background-subtracted long BATSE bursts after peak alignment, with peak time suppressed. Rates between 20 and 100 keV are shown for 400 bursts lasting longer than 2 s (stars) and 200 medium bursts (triangles) with 30 s as the dividing duration. Left plot shows count rates per burst, right plot is the fraction of peak flux at a given time.

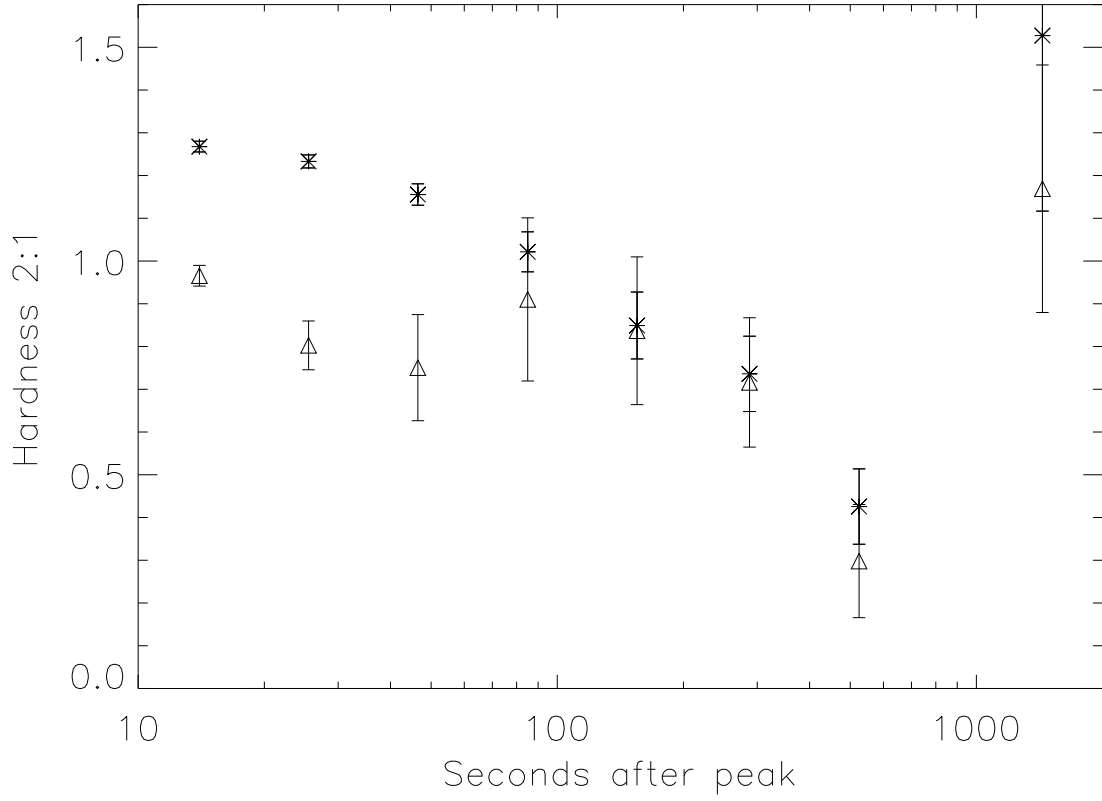


Fig. 5.— Hardness ratios (50-100 keV/20-50 keV) for long (> 2s) bursts (stars), bursts with durations between 2 and 30 s(triangles).

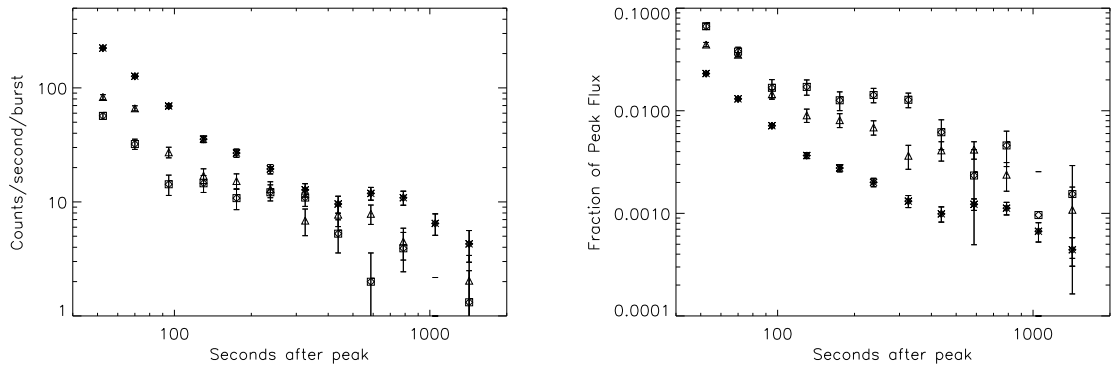


Fig. 6.— Three groups of long (> 2 s) bursts separated by the brightness of their peak emission. The left plot shows the count rate between 20 and 100 keV per burst of the emission from $t_0 + 40$ s onwards, the right shows the magnitude of this emission relative to the intensity at the peak. The stars are the brightest bursts, the triangles intermediate, the squares the dimmiest.

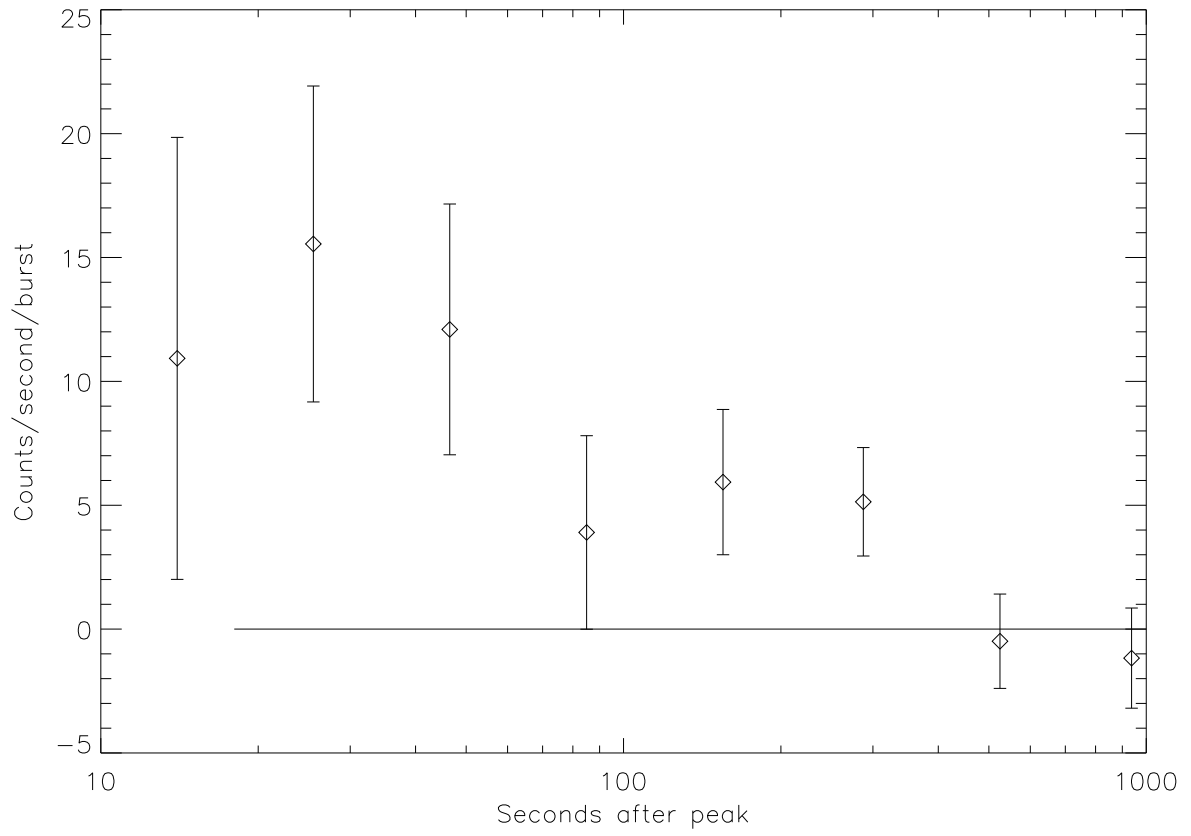


Fig. 7.— Lightcurve for 100 short (< 1 s) summed background-subtracted BATSE bursts after peak alignment, with peak time suppressed.

Table 1: Tails and afterglows of individual GRBs

Tailed					Tailless				
GRB date	X	O	I	R	GRB date	X	O	I	R
970111	N	N		N	970508	Y	Y	Y	Y
971024		N			971214	Y	Y	Y	N
980329	Y	Y	Y	Y	980611	N			
980613	Y	Y	N		990520		N		
980703	Y	Y	Y	Y					
990506	Y	N							
991216	Y	Y	Y	Y					